Postcritical behaviour of thin aluminium plates

Autor(en): **Fernezelyi, Sándor**

Objekttyp: **Article**

Zeitschrift: **IABSE reports = Rapports AIPC = IVBH Berichte**

Band (Jahr): **49 (1986)**

PDF erstellt am: **23.07.2024**

Persistenter Link: https://doi.org/10.5169/seals-38281

Postcritical Behaviour of Thin Aluminium Plates

Comportement postcritique des tôles minces en aluminium

Überkritisches Verhalten dünner Aluminiumbleche

Sándor FERNEZELYI
Civil Engineer
Hungalu Eng. and Dev. Centre
Budapest, Hungary

S. Fernezelyi, born 1942, received his civil engineering degree and Ph.D. at the Technical University of Budapest. For eighteen years he was involved in problems of load-bearing aluminium structures. He is the designer of several large span aluminium roofs. S. Fernezelyi is now responsible for the engineering activity of the Hungarian Aluminium Co.

SUMMARY

According to our experiments, the structural components made of thin plates and loaded in unidirectional and uniform compression, lose their load-bearing capacity so that a plastic mechanism develops within which the lines of the plastic hinges are curved. Assuming a crushing profile that adequately approximates to the reality and considering the difference between the patterns of both the elastic and the plastic deformations, and also, considering the initial curvature of the plate, the value of ultimate load can be determined as a function of the plate's slenderness.

RÉSUMÉ

Nos essais ont montré que les éléments en tôle mince soumis à une compression uniforme perdent leur capacité portante par formation d'un mécanisme de ruine dans lequel les lignes de rupture plastique sont courbes. A l'aide d'un modèle de rupture proche de la réalité, en tenant compte des différences entre les valeurs élastique et plastique des déplacements et en considérant aussi les déformations initiales de l'élément, la valeur de la charge ultime de la plaque peut être déterminée en fonction de son élancement.

ZUSAMMENFASSUNG

Unsere Versuche haben gezeigt, dass die durch gleichmässigen Druck in einer Richtung belasteten dünnen Blechelemente ihre Tragfähigkeit verlieren, indem sich ein plastischer Mechanismus ausbildet, dessen Fliesslinien gebogen sind. Wenn wir ein der Wahrheit nahe stehendes Bruchbild annehmen und den Unterschied zwischen den elastischen und plastischen Verformungsmustern sowie die Anfangskrümmung des Bleches berücksichtigen, kann der Wert der maximalen Last als Funktion der Blechschlankheit bestimmt werden.

1. INTRODUCTION

Corrugated sheets being of wide use in building construction are made of substantially thinner material than that used in load-bearing structures in general. In spite of the fact that increased attention has been focused on post-critical behaviour of plates [1], [2], rather limited experimental and theoretical knowledge is still available concerning such ranges of width-to-thickness ratio. This is particularly true in the case of aluminium plates.

In order to establish the ultimate load, the form of collapse, the shape of the plastic mechanism should previously be determined. Most of the authors [3], [4], [5] assume that lines of the plastic hinges are straight, so that the shape of the plastic mechanism involves two triangles and two trapezoids (See Fig. 3/a). It is also assumed [5] that ultimate strength of the plate can be found as the intersection of a post-buckling loading curve with a plastic unloading line. However, experimental data have not fully confirmed the theoretical results [6].
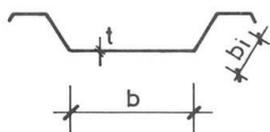
2. DESIGN OF EXPERIMENTS

Figure 1.

In order to expand our data base, a far-flung experimental project has been recently accomplished. Characteristic cross-section of the samples are shown on Fig.1. Eccentric compression was used for loading. The samples were prepared with the use of standard corrugated sheets manufactured by the Hungarian Aluminium Corporation. For the trial runs, samples of various length, width, thickness and alloy were used. In all, 78 samples representing 22 types, were tested. Thus, our results are considered fairly appropriate to draw conclusions of general character.

Our investigations included testing of:

- initial imperfections;
- critical buckling load experienced during the tests;
- post-critical behaviour, and the ultimate load of the plate;
- interaction between the general and local buckling, in order to determine the ultimate load of the entire structural component.

The results were given in detail elsewhere [7], therefore, we shall herein use only experimental results concerning initial imperfections and the ultimate load of the plate.

We consider our experimental result a substantial one, namely that, in all cases, the shape of the plastic mechanism is as shown on Fig.2, i.e. the lines of plastic hinges are curved!

3. RANGE OF INVESTIGATIONS AND THE INITIAL ASSUMPTIONS

For comparison with previous experiments we have limited the field of investigations and made the following initial assumptions (for the applied notes, see Fig.1):

(i) the sections are cold formed, their thickness is constant, i.e. $t = const.$;

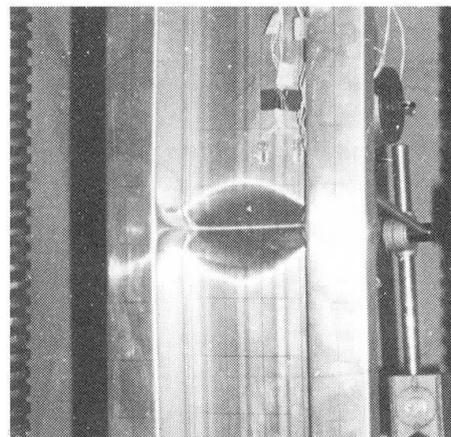(ii) the plates are "extremely" thin, where slenderness ratio of one component plate is: $b/t > 80$;

Figure 2.

(iii) slenderness ratio of the connecting plates is much lower, i.e. $b_i < 1/2 \, b$. Thus, buckling of such plates has no effect on the loading capacity of the entire section. Otherwise, the widest plate can be considered being simple supported;

(iv) the load is such as to cause uniform displacement at the loaded edges;

(v) the unloaded edges are stress free, thus, they do not remain straight;

(vi) collapse of the section shall always take place through the collapse of the widest plate component;

(vii) local deformation of the unloaded edges has no significant effect on the collapse load.

Our experiments demonstrated that collapse of the component plate is frequently associated with simultaneous collapse of the edges. The value of yield stress is assumed to develop at the unloaded edges.

(viii) lines of the plastic hinges are curved.

4. SHAPE OF THE PLASTIC MECHANISM

Figure 3/a shows that shape of the plastic mechanism which has been normally assumed in the literature, compared to Fig. 3/b which in turn, shows the shape proposed by us in conformity with the experimental results.

The function that describes the surface (according to the co-ordinate system shown in Fig. 3/b) is the following:

Figure 3/a.

Figure 3/b.
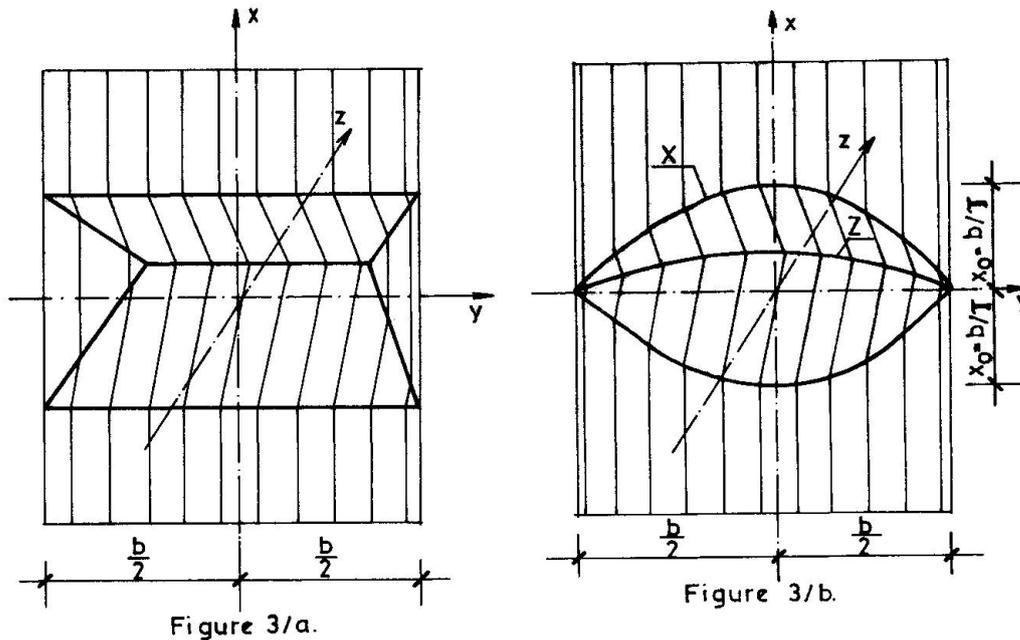
$$\frac{x}{X} + \frac{z}{Z} = 1 \tag{1}$$

Herein, "X" and "Z" represent functions of the curves which describe the lines of the plastic hinges and determine the character of the buckled shape.

Perpendicular sections of the surface shall create straight lines. (This proposed shape is the product of an approximation since the line described by the "X" function does not lie in the reference plane, however, showed that the resultant neglect is of no significance.)

The "X" and "Z" curves which determine the surface as well as the in-plane displacement (δ) are not independent.

$$X = \frac{z^2 - \delta^2}{2\delta} \tag{2}$$

The angle experienced at the lines of the plastic hinges shall be:

$$\varphi_v = tg^{-1} \frac{2\delta z}{z^2 - \delta^2} \tag{3}$$

Assuming existence of discrete angles in the plane of the other main curvature, its value can be given as:

$$\Delta\varphi_H = \left\{ 2\delta x_i \left[2zz'^2 \frac{z^2 - 3\delta^2}{(z^2 - \delta^2)^3} - z'' \frac{z^2 + \delta^2}{(z^2 - \delta^2)^2} \right] - z'' \right\} \cos \varphi_v \cdot \Delta x \tag{4}$$

where: x_i gives the locality of the investigated horizontal section
        Δx distance between horizontal sections

With the use of the above findings and by taking notice of the yield conditions, we can determine the external and internal part of the plastic work effected during deformation.

5. STRESS DISTRIBUTION

Based on equal external and internal plastic work and after certain mathematical transformations, we can describe the distribution of stress:

$$\frac{n}{n_{pl}} = \frac{t}{4} \left\{ \left[1 - \left(\frac{n}{n_{pl}}\right)^2 \right] \frac{2}{\delta} \left[tg^{-1} \frac{2\delta z}{z^2 - \delta^2} \right] + \right.$$

$$\left. + \left[1 - \frac{1}{2}\left(\frac{n}{n_{pl}}\right)^2 \right] \frac{1}{2\delta^2} \left[zz'^2 \frac{z^2 - 3\delta^2}{z^2 - \delta^2} - \frac{z''}{2}\left(3z^2 - \delta^2\right) \right] \right\} \tag{5}$$

where: $n = \sigma.t$ normal stress
        $n_{pl} = \sigma y.t$ yield stress

It can be seen that stress distribution depends solely on the rate of in-plane compression (δ) and the function which determines the shape of the yield mechanism (Z).

If we consider a model of plastic-rigid material then the resultant in-plane compression in the plastic mechanism, i.e.

$$\delta = \delta_o = \text{constant}$$

shall be indentical with the total compression (δ_o). Assuming a constant cross-section throughout (see condition iv.), this creates a geometric contradiction in the vicinity of the edges. We shall then obtain a solution well in conformity with the experimental results by taking into consideration the elastic compressions, as well:

$$\delta_o = \delta_e + \delta = \text{constant}$$

where: δ_e elastic compression

Beyond the geometric data the elastic compression shall depend on the stress distribution and, if we consider proportions of the shape of the plastic mechanism, the plastic compression shall be:

$$\delta = \frac{W_{pl}^2 \, \pi}{2b} \, \frac{1-n/n_{pl}}{1-n_o/n_{pl}} \qquad (6)$$

where: n_o value of stress at the axis of symmetry

W_{pl} highest value of out-of-plane displacement within the assumed plastic mechanism

If we consider the omissions that can be made concerning small angles, the relation (5) can be significantly simplified. Let's assume that function "Z" is described in the following form:

$$Z = W_{pl} \cdot \eta \cdot \left(\frac{\pi y}{b} \right) \qquad (7)$$

This, and the substitution of the eqn. (6) into the eqn. (5) and having implemented the necessary reductions, we obtain an explicit function that describes the curve of stress distribution:

$$\frac{n}{n_{pl}} = \left[1 - \left(\frac{n}{n_{pl}} \right)^2 \right] \frac{t}{W_{pl} \eta} + \left[1 - \frac{1}{2} \left(\frac{n}{n_{pl}} \right)^2 \right] \cdot$$

$$\cdot \frac{(1-n_o/n_{pl})^2}{(1-n/n_{pl})^2} \left(\frac{1}{2} \eta \eta'^2 - \frac{3}{4} \eta^2 \eta'' \right) \frac{t}{W_{pl}} \qquad (8)$$

It is evident that by knowing the function η, we can determine the relation between the out-of-plane displacement and the stress distribution. Since the integral of the stresses constitutes the upper limit of the ultimate load, and according to the theory of plasticity, its minimum value approaches mostly the real value of load bearing capacity, we obtain the following variational problem:

$$\int_b \frac{n}{n_{pl}} \, dy = min! \qquad (9)$$

Since the exact mathematical solution of this task involves extreme difficulties, we resort to an approximation. We have investigated eight functions which met the requirements of boundary conditions and came to the following conclusions:

- a partial consideration of the elastic displacements as opposed to the purely rigid-plastic model shall cause only an insignificant change with respect to the ultimate load, however, the shape of yield mechanism becomes more realistic;

- in case of the curvilinear plastic mechanism (see Fig. 3/b) we obtain a significantly (i.e. by 22 %) lower value for the ultimate load than in case of the plastic mechanism containing straight lines. (See Fig. 3/a). Therefore, it stands closer to reality;

- the choice of curved line has a relatively small effect; the comparison of the different curves yields a variance lesser than 10 %;

- from among the considered trial-functions, the second order parabola, being of the form of

$$Z = 0,955 \, W_{pl} \, [1-(2y/b)^2] \qquad (10)$$

resulted in the minimum value. Thus, it describes the shape of the plastic mechanism with a grade of precision that meets the requirements of engineering calculations.

Having repeated the calculation concerning the eqn. (8) applying numeric approaches, the resultant curves of stress distribution illustrated in Fig.4, representing various kinds of different out-of-plane displacements. Also, with respect to the case of $W_{pl}/t = 5$, we demonstrate a stress distribution which can be calculated on the basis of a straight line plastic mechanism.
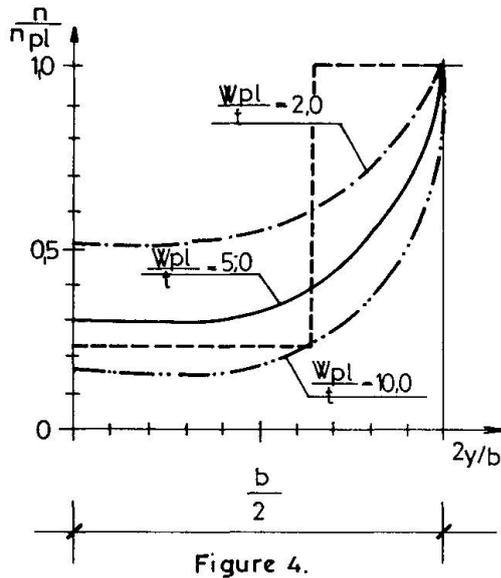

Figure 4.

6. PLASTIC UNLOADING LINE

By means of a repeated numeric integration, the values of the upper limit of the ultimate load could be determined, with respect to the values of out-of-plane displacement. Thus, we could develop the plastic unloading line (see Fig.5).

In order to find a more manageable form, we sought for an approximating function which should describe with sufficient precision the numerically determined values.

We found that:

$$\frac{P_u}{P_{pl}} = \frac{1}{1+0,3W_{pl}/t} \tag{11}$$

where: P_u ultimate load of the plate
       P_{pl} yield load of short plate

The formula shall provide the numerically determined values within a range of ±1.7 %.

7. ELASTIC DEFORMATION LINE

The relation between the load and elastic deformation is considered being in conformity with the literature and formulated according to our investigations:

- in case of initially flat plate:

$$\frac{P}{P_{pl}} = \frac{\sigma_{cr,p}}{\sigma_y} \left[\frac{1-\nu^2}{8} \left(\frac{W_e}{t} \right)^2 + 1 \right] \tag{12}$$

$\sigma_{cr,p}$ critical buckling stress
ν Poisson's ratio
W_e elastic out-of-plane displacement

- when the characteristic value of the eccentricity is:

$$\alpha = W_o/t$$

$$\frac{P}{P_{pl}} = \frac{\sigma_{cr,p}}{\sigma_y} \left\{ \frac{1-\nu^2}{8} \left[\left(\frac{W_e}{t} \right)^2 - \alpha^2 \right] \right\} + \frac{W_e/t+\alpha}{W_e/t} \tag{13}$$

8. ULTIMATE LOAD

The intersection of the plastic unloading line with the load/elastic displacement curve provids the upper limit of ultimate load (see Fig.5).

The real load/displacement path can be distributed to three phases:

I.   elastic phase;
II.   phase is where plasticity sets in. Here, the elastic pattern of displacements transforms in to the plastic pattern of displacements;
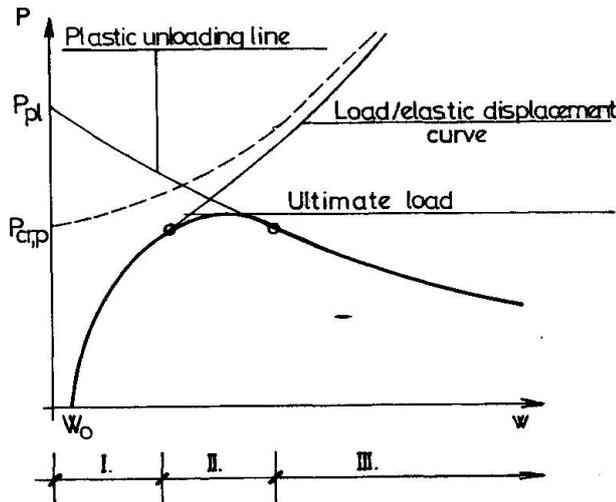III. plastic phase.

Figure 5.

It can be seen that extremum of the real curve (wich indicates the value of the ultimate load) is situated below the intersection. In order to assess this effect, we present a vertical cross-section of both the elastic pattern of displacements (Fig.6/a) and that of the plastic one, (Fig. 6/b).

Figure 6.

Assuming that the transformation should take place at an identical value of in-plane displacement (and using the legend applied in Figure 6), we can determine the following relation between the characteristic values of out-of-displacement:
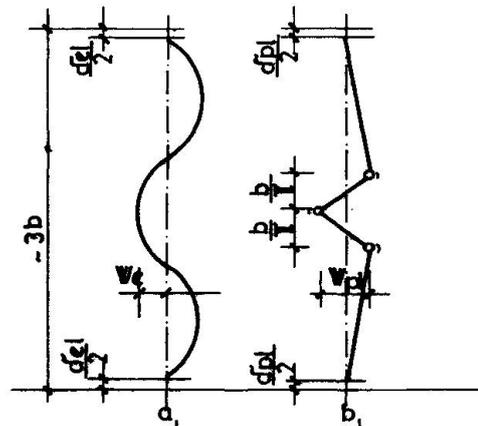
$$W_{pl} = W_e \sqrt{\frac{3\pi/4}{\pi+1/(b+4/\pi)}} = 1,50W_e \tag{14}$$

While comparing the displacements, the above relation is used as a correction factor. Thus, by equating the plastic displacement calculated from the eqn. (11) with the elastic displacement derived from the eqn. (12), and taking into consideration the correction (14), we obtain the relation between the slenderness of the initially flat plate and its ultimate load:

$$\overline{\lambda}_{po} = \sqrt{\frac{(1-\overline{P})^2 + 1,78\overline{P}^2}{1,78\overline{P}}} \tag{15}$$

where: $\overline{\lambda}_{po}$ slenderness of the initially flat plate
       $\overline{P} = P_u/P_{pl}$ relative ultimate load

If we perform the same comparison using the formula of load/elastic displacement (13) which takes into consideration the initial eccentricity as well, furthermore, if we assume, in conformity with our experimental results, the value of the latter in the form of:

$$\alpha = \frac{W_o}{t} = A\left(\frac{b}{t}\right)^2 = A_1 \cdot \overline{\lambda}_p^2 \qquad , \quad \overline{\lambda}_p = \sqrt{\sigma_y/\sigma_{cr}} \tag{16}$$

where: $A_1 = A \dfrac{\pi E k}{12(1-\nu^2)\sigma_y}$

The relation between slenderness of the plate and the ultimate load shall be the following:

$$\overline{\lambda}_p{}^2 = \overline{\lambda}_{po}{}^2 - \frac{A_1}{8,79\overline{P}} \overline{\lambda}_p{}^4 - \frac{0,45A_1}{1\overline{P}} \overline{\lambda}_p{}^2 \tag{17}$$

where: $\overline{\lambda}_p$ slenderness of the initially imperfect plate
      $\overline{\lambda}_{po}$ slenderness of the plate of equal loadability which was, however, plane initially.

9. EXPERIMENTAL RESULTS

Fig.7 illustrates the curves calculated with the use of formulas (15) and (17). The latter was calculated with respect to the initial curvature being of a characteristic value of $A_1 = 0.141$. This value was obtained on the basis of results of evaluation of 62 samples.
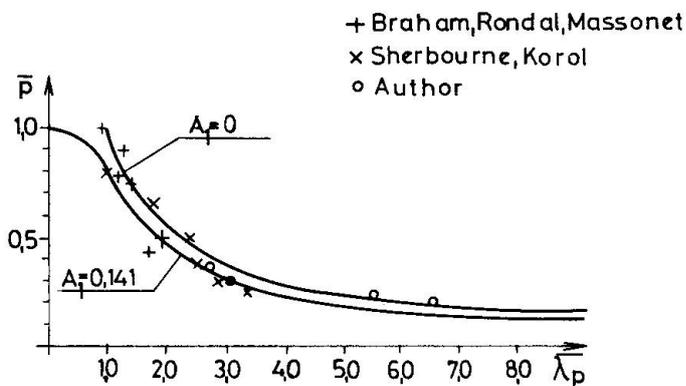
Figure 7.

The values of ultimate load obtained through experiments, were plotted in the figure, where several well-comparable measurement data can be observed, as well. It can be established that the theoretically determined curve fits quite well with the experimental results.

10. IMPLEMENTED STRUCTURES

This process was used to control calculations concerning a roof structure of 30 meters span and manufactured from 1 mm thick plate. The roof structure was subjected to a full scale loading test. The difference of the measured and calculated values remained within a highly satisfactory range of 2.5 %.

REFERENCES

1. WILLIAMS,D.G., AALAMI,B., Thin Plate Design for In-plane Loading. Granada, London, 1979.
2. RHODES,I., WALKER,A.C., Thin-Walled Structures. Granada, London, 1980.
3. DAVIES,P., KEMP,K.O., WALKER,A.C., An Analysis of the Failure Mechanism of an Axially Loaded Simply Supported Steel Plate. Proc.ICE.Part 2. Vol.59.
4. IVANYI,M. Yield Mechanism Curves for Local Buckling of Axially Compressed Members. Periodica Politechnica. C.E. Vol.23. 1979.
5. KOROL,R.M., SHERBOURNE,A.N., Strength Predictions of Plates in Uniaxial Compression. I.ASCE. Vol.98. St9. Sept.1972.
6. SHERBOURNE,A.N., KOROL,R.M., Post-Buckling of Axially Compressed Plates. I.ASCE. Vol.98. St9. Oct.1972.
7. FERNEZELYI,S., Load-bearing capacity of thin aluminium plates. Experimental Investigation. Magyar Aluminium. (Prepared for publication, in Hungarian.)